Journal of Undergraduate Chemistry Research, **2023**, 22(4), 86

STRUCTURAL PROPERTIES OF A THREE-DIMENSIONAL INORGANIC COORDINATION NETWORK, $K_5Na[Pr_2(SO_4)_6]$

Emma Rust[*], Daniel Rios[*], Jackson Turner[*], William Best[*,#], Emory Brandon[*], Braeden Myers[*], Matthias Zeller[+], and Ralph A. Zehnder[†]

Department of Chemistry and Biochemistry, Angelo State University, San Angelo, TX 76909
[#]Central High School, San Angelo, TX 76901
[+]Department of Chemistry, Purdue University, West Lafayette, IN 47907

Abstract

Modifying well established slow diffusion procedures at room temperature to produce metal-organic coordination polymers led to the creation of the inorganic title compound, $K_5Na[Pr_2(SO_4)_6]$. It is isomorphous to a series of $K_6[Ln_2(SO_4)_6]$ (Ln = La, Ce, Pr) and $K_5Na[Ln_2(SO_4)_6]$ (Ln = Ce, Nd, Sm, Eu) coordination networks that were previously reported. All crystallize in the monoclinic crystal system with space group *C*2/*m*. We compare the structural properties of PrO_{10}-coordination polyhedra between $K_5Na[Pr_2(SO_4)_6]$ and the published $K_6[Pr_2(SO_4)_6]$ species. $K_5Na[Pr_2(SO_4)_6]$ assembles as a three-dimensional network. PrO_{10}-polyhedra form binuclear Pr_2O_{18}-polyhedra via edge sharing. These are infinitely linked via SO_4^{2-}-ions and expand within the *ab*-plane. The resulting 2D-layers are linked along the *c*-axis by 9 and 8 -coordinate K^+-ions as well as 6-coordinate Na^+-ions

[†]Corresponding author: ralph.zehnder@angelo.edu * Undergraduate researchers and co-authors
Keywords: nuclear waste, lanthanides, actinides, coordination polymers, inorganic compounds
Submitted: August 22, 2023 Accepted: August 30, 2023 Published: September 15, 2023

Introduction

Nuclear energy is expected to adopt a more significant role as the climate crisis intensifies. Energy needs must be met amid efforts regarding the reduction of carbon emissions.[1-4] The safe storage and/or reprocessing of nuclear materials has been under intense investigation for decades.[5-9] The treatment of nuclear waste materials with ground glass at high temperatures (vitrification process) and integration into ceramics are currently the main avenues for the processing of radionuclides stemming from dismantling nuclear weapons, nuclear medicine, research, and spent nuclear fuels.[5, 10] Concerns about the migration of radioisotopes within waste matrices and their potential leaching and escaping into the environment have led to the desire of finding alternatives for the fixation of such radioisotopes.[11-13]

The formation of stable matrices by integrating the radioactive elements in form of coordination centers in inorganic or metal-organic coordination networks might present an alternative path for the immobilization of radioisotopes.[14-16] Due to the chemical similarities between trivalent lanthanide (Ln) elements and their actinide (An) counterparts, namely trans uranium actinides (Pu, Am, Cm, etc.), 4*f*-elements have an extensive history of being utilized as surrogates for the targeted 5*f*-analogs.[15, 17-19] Our efforts have evolved around the creation of lanthanide coordination polymers that integrate purely inorganic entities as well as compounds that incorporate organic ligands as linkers between metal centers within coordination networks.[20-23] Once a synthetic procedure is well established utilizing the 4*f*-elements, it is feasible to replicate it with selected actinides.

For this purpose, we created a neodymium (Nd) glutarate (glut) terephthalate (TP) coordination polymer of formula $Nd_2(Glut)_2(TP)(H_2O)_4 \bullet 17H_2O$, using a hydrothermal synthetic procedure.[21] Later we obtained this compound after developing suitable slow diffusion methods at room temperature (RT) by reacting $NdCl_3$ dissolved in water with a mixture of Na_2Glut and Na_2TP dissolved in equal amounts of tetrahydrofuran (THF), ethanol (EtOH), and water. This approach at RT assisted us in extending the synthesis to several isomorphous lanthanide analogs (La, Ce, Pr, Sm), which had failed to form applying the hydrothermal route. By replacing the terephthalate entity with its bromoterephthalate derivative (TPBr), we created an isomorphous series of $Ln_2(Glut)_2(TPBr)(H_2O)_4 \bullet XH_2O$ (Ln = La, Ce, Pr, and Nd, X = values between 4 and 16) applying again slow diffusion procedures at RT. This series of structurally identical *f*-element glutarate bromoterephthalate compounds will be discussed in an upcoming manuscript. Replacing the aqueous solution of the lanthanide starting materials, $LnCl_3$, with $Ln_2(SO_4)_3$ resulted in the formation of the title compound, $K_5Na[Ln_2(SO_4)_6]$, as a side product.

Experimental Methods

2-Bromoterephthalic acid, potassium hydroxide (Thermo Scientific), praesodymium(III) sulfate (Alfa Aesar), glutaric acid, THF (Acros Organics), sodium chloride, and anhydrous ethanol (Fisher Science Education), were used as received and without further purification.

Preparation of K_2Glut 80 mM in THF/EtOH/H_2O

3.169 g (24 mmol) of glutaric acid (H_2Glut) were dissolved in 100 mL of DI-H_2O. 2.693 g of KOH (48 mmol) were added, which resulted in a clear colorless homogeneous solution. 100 mL of THF and 100 mL of EtOH were added to make up the final solution (80 mM).

Preparation of K_2TPBr 40 mM in THF/EtOH/H_2O

2.94 g (12 mmol) of H_2TPBr were suspended in 100 mL of DI-H_2O. Then 1.36 g of KOH (24 mmol) were added, which resulted in a clear colorless homogeneous solution. 100 mL of THF and 100 mL of EtOH were added to make up the final solution (40 mM).

Preparation of 2:1 K_2Glut / K_2TPBr solution in THF/EtOH/H_2O (40 mM and 20 mM respectively)

50 ml of K_2Glut solution in THF/EtOH/H_2O (80 mM) were

mixed with 50 ml of K_2TPBr solution in THF/EtOH/H_2O (40 mM).

Synthesis of $K_5Na[Pr_2(SO_4)_6]$ (**1**)

Using a VWR Clip Tip Finn pipette, a 7 mL scintillation vial was filled with 3 mL of the K_2Glut/K_2TPBr solution (molar ratio 2:1) (40 and 20 mM, resulting in amounts of 0.12 mmol, 0.06 mmol respectively) in THF/EtOH/H_2O. 0.061 g of NaCl were added (1.0 mmol) and the mixture was shaken. Using the Finn pipette, 1 mL of a 21 mM aqueous $Pr_2(SO_4)_3$ solution (0.021 mmol) was placed at the bottom of the 7 mL scintillation vial, creating two layers of solutions. The vial was capped and left undisturbed for the two layers to mix slowly via diffusion.

Within three days green and colorless single crystals grew in form of plates and rectangular blocks. Single crystal X-ray diffraction data helped to identify the plates as $Pr_2(Glut)_2(TPBr)(H_2O)_4 \bullet XH_2O$, and the blocks to be the title compound $K_5Na[Ln_2(SO_4)_6]$ (**1**).

Single Crystal X-ray Structure Determination

Data for single crystals of **1** were collected on a Bruker AXS D8 Quest three circle diffractometer with a fine focus sealed tube X-ray source using a Triumph curved graphite crystal as monochromator and a PhotonII charge-integrating pixel array (CPAD) detector and an Oxford Cryosystems low temperature device. A colorless fragment with approximate dimensions of 0.05 × 0.12 × 0.19 mm was mounted on a Mitegen micromesh mount in a random orientation. Data were collected from a shock-cooled single crystal at 150(2) K. Data were collected, reflections were indexed and processed, and the files scaled and corrected for absorption using APEX4[24] and SADABS.[25] The space groups were assigned using XPREP within the SHELXTL suite of programs[26, 27] and the structure was solved by dual methods with ShelXT[28] and refined by full-matrix least-squares methods against F^2 using SHELXL-2019/2.[28, 29] All atoms were refined with anisotropic displacement parameters.

The crystal data and summary of data collection and refinement for the title compound are provided in Table 1.

Crystallographic data, CCDC 2288663, was deposited with the Cambridge Crystallographic Data Centre and can be obtained free of charge via www.ccdc.cam.ac.uk/data_request/cif.

Results and Discussion

Several isomorphous $K_6[Ln_2(SO_4)_6]$ (Ln = La, Ce, and Pr) and $K_5Na[Ln_2(SO_4)_6]$ (Ln = Nd, Sm, and Eu) salts have been presented as recently as last year by Sørensen *et al.*[30, 31] as well as by Eriksson *et al.* in 2003 ($K_5Na[Ce_2(SO_4)_6]$).[32] While $K_5Na[Pr_2(SO_4)_6]$ is isomorphous to these compounds, to our knowledge, it has not been described in the literature so far. All these species crystallize in the monoclinic crystal system with space group *C*2/*m*.

1 and its previously published structurally similar analogs are purely inorganic coordination networks which awakened our interest as they may be candidates for further investigations regarding their potential use as surrogate nuclear waste matrices. Our aim is to simplify the syntheses of targeted 4*f*-element products to have a protocol in place for replicating the refined approach with the early trans-uranium elements plutonium and americium. Most recently we have begun the development of synthetic protocols to obtain **1** as a pure compound without employing the lanthanide starting materials Sørensen *et al.* utilized, i.e. ($Ln(CF_3SO_3)_3$), since it would be rather challenging to replicate these experimental setups with Pu and Am.

In their manuscripts Sørensen and coworkers focused on structural changes, mostly regarding the LnO_{10}-coordination polyhedra, within the series of isomorphous $K_6[Ln_2(SO_4)_6]$/$K_5Na[Ln_2(SO_4)_6]$ compounds they prepared. They describe their synthetic reactions to include both alkali metal ions, K^+ and Na^+ in the solutions used. However, they only observed the lanthanides with larger ionic radii assemble as $K_6[Ln_2(SO_4)_6]$ (La, Ce, and Pr). The smaller Ln^{3+} metal centers (Nd, Sm, Eu) seem to alleviate the increased strain on the crystal lattice by inserting smaller Na^+-ions into the lattice for one sixth of the K^+-ions.

Eriksson's and our team show that for the larger lanthanides, Ce and Pr, the $K_5Na[Ln_2(SO_4)_6]$ counterparts can also be obtained. Thus, these two structures contribute complementary data to Sørensen's project, who addressed in their article that it seems rather unlikely for the $K_6[Ln_2(SO_4)_6]$ counterparts to form with the smaller Ln^{3+} ions, as the lattice provides less space for all K-metal centers to fit into their positions. Herein we analyze the structural properties pertaining to the 3D-crystal lattice of **1** and compare average bond lengths within coordination polyhedra with the reported ones.

Table 1. Crystal Data and Summary of Data Collection and Refinement for Compound **1**

Formula	$K_5Na[Pr_2(SO_4)_6]$ (**1**)
Fw (g/mol)	614.38
a (Å)	9.1740(7)
b (Å)	16.2888(15)
c (Å)	7.6784(7)
α (°)	90
β (°)	110.926(4)
γ (°)	90
V (Å^3)	1071.73(16)
Crystal system	monoclinic
Space group	*C*2/*m*
Z	2
D_c (Mg•m^{-3})	3.336
μ (mm^{-1})	6.184
F(000)	1024
Crystal size (mm^3)	0.190 x 0.120 x 0.050
Radiation	MoKα (λ = 0.71073 Å)
2Θ range for data collection/°	2.4997 to 33.0415
T (K)	150 (2)
Refln. Tot.	13177
Refln. Indep.	2116
Refln. I>2σ(I)	1937
R_{int}	0.0410
R1 (I>2σ(I))	0.0218
wR2 (I>2σ(I))	0.0486
Data/restraints/parameters	2116/0/95
Goodness-of-fit on F^2	1.072
Largest diff. peak/hole / e Å^{-3}	1.519/-1.333

1 assembles as a three-dimensional (3D) coordination network. Figure 1 presents the top view onto the *ab*-plane of this structure. Figure 2 illustrates how 2D-layers of binuclear Pr_2O_{18}-polyhedra are infinitely linked via SO_4-tetrahedra and propagate within the *ab*-plane. The Pr_2O_{18}-polyhedra are composed of two PrO_{10}-polyhedra that are linked via edge sharing. There are two crystallographically distinct potassium metal centers, K(1) and K(2) as well as sulfate S-atoms, S(1) and S(2). Individual Pr^{3+}-ions are surrounded by six sulfate ligands, of which four are coordinated in a bidentate manner, and the other two in a monodentate fashion. The Pr-atoms lie on a mirror plane that is parallel to the *ab*-plane. Closer inspection of the Pr_2O_{18}-polyhedra reveals that two of the four sulfate entities binding in a bidentate manner stem from $S(2)O_4$-tetrahedra that are inserted between the corners of the two PrO_{10}-coordination spheres and exhibit bidentate coordination to both PrO_{10}-polyhedra. Thus, besides linked together by edge sharing the PrO_{10}-entities are further connected by the two $S(2)SO_4$-tetrahedra, which are dissected by a mirror plane that coincides with the *ac*-plane (Figure 3). In Table 2 we list all compounds' average bond-distances of the LnO_{10}-polyhedra, as well as their bond valence sums to confirm their trivalent state in these crystal structures. For calculating the bond valence sums we used equation 1, which was proposed by Brown and Altermatt:[33]

$$V_i = \sum s_{ij} = \sum \exp[(R_0 - r_{ij})/b] \qquad (1)$$

Here, V_i represents the calculated oxidation state of central-atom i of a coordination polyhedron; s_{ij} and r_{ij} stand for the valence and the length of the individual bonds between central atom i and ligand atom j; R_0 is the distance for a given cation-anion pair that has been empirically elucidated and can be found in the literature;[34] b represents a "universal parameter"[35] and generally is equal to 0.37.[36] The sum of all valences is denoted with V, which is an approximation of the value for the formal oxidation state.[37]

The bond distances of the 10-coordinate Pr-metal centers in $K_5Na[Pr_2(SO_4)_6]$ and Sørensen's $K_6[Pr_2(SO_4)_6]$ compare very well. They are basically identical. For the Ce-pair between Erikksson's $K_5Na[Ce_2(SO_4)_6]$ and Sørensen's $K_6[Pr_2(SO_4)_6]$, very small differences can be observed. Nevertheless, the average bond-distances for Ln-O_{10} in these two pairs are identical and slightly decrease from 2.604 to 2.584 Å moving from the Ce-compounds to the Pr-equivalents. This is not surprising with the ionic radii slightly

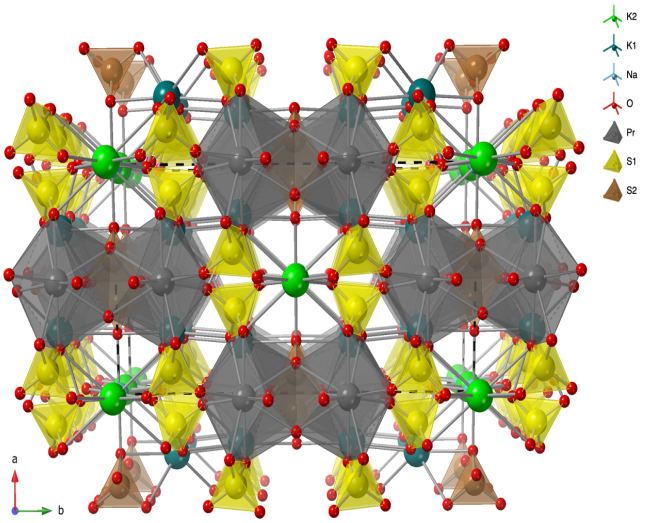

Figure 1: Top view onto the *ab*-plane of the 3D-coordination network in **1**.

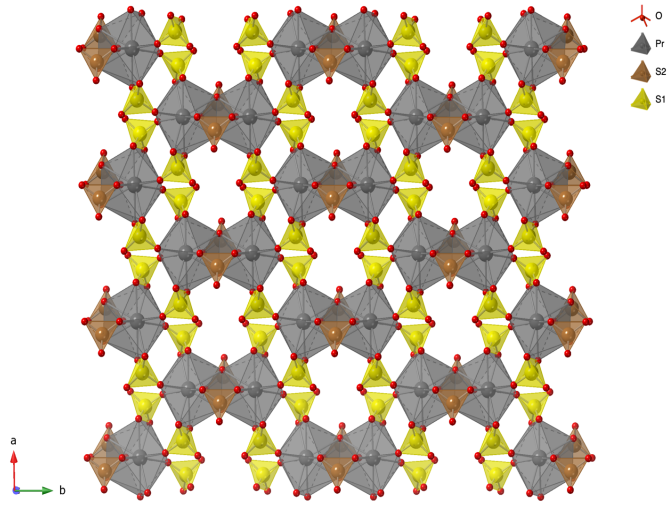

Figure 2. Infinate propagation of Pr_2O_{18}-coordination polyhedra interlinked with SO_4-tetrahedra within the *ab*-plane. K and Na -metal centers removed for clarity.

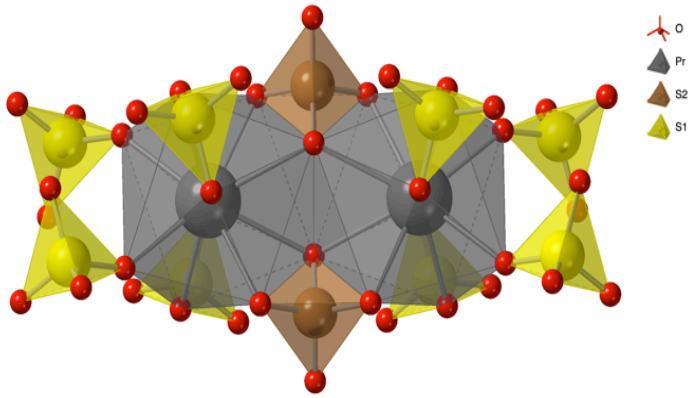

Figure 3. Coordination environment of a binuclear Pr_2O_{18}-coordination polyhedron which is composed of two edge sharing PrO_{10}-polyhedra. Each Pr-metal center is bound to six sulfate entities. Four are coordinated in a bidentate fashion and two in a monodentate style. Two of the four sulfate entities binding in bidentate manner stem from $S(2)O_4$-tetrahedra that are inserted between the corners of the two PrO_{10}-coordination spheres exhibiting bidentate coordination to both PrO_{10}-polyhedra.

Table 2. Comparing average bond distances of LnO_{10}-coordination polyhedra in $K_6[Ln_2(SO_4)_6]$[31] and $K_5Na[Ln_2(SO_4)_6]$, and bond valence sums for individual Ln(III)-ions.

$K_6[La_2(SO_4)_6]$ measured at 100 K	Average La-O distances: 2.614 Å Valence sum: 2.901 Sørensen *et* al.[31]	$K_5Na[Nd_2(SO_4)_6]$ measured at 100 K	Average Nd-O distances: 2.571 Å Valence sum: 2.784 Sørensen et al.[31]
$K_6[Ce_2(SO_4)_6]$ measured at 100 K	Average Ce-O distances: 2.604 Å Valence sum: 2.785 Sørensen *et* al.[31]	$K_5Na[Ce_2(SO_4)_6]$ measured at 173 K	Average Ce-O distances: 2.604 Å Valence sum: 2.784 Erikkson *et* al.[32]
$K_6[Pr_2(SO_4)_6]$ measured at 100 K	Average Pr-O distances: 2.585 Å Valence sum: 2.756 Sørensen *et* al.[31]	$K_5Na[Pr_2(SO_4)_6]$ (**1**) measured at 150 K	Average Pr-O distances: 2.583 Å Valence sum: 2.776 This work
$K_5Na[Sm_2(SO_4)_6]$ measured at 100 K	Average Sm-O distances: 2.545 Å Valence sum: 2.817 Sørensen *et* al.[31]	$K_5Na[Eu_2(SO_4)_6]$ measured at 100 K	Average Eu-O distances: 2.534 Å Valence sum: 2.714 Sørensen *et* al.[31]

decreasing moving from Ce to Pr.

Thus, the size of the LnO_{10}-coordination polyhedra is similar for $K_5Na[Pr_2(SO_4)_6]$ and $K_6[Pr_2(SO_4)_6]$. The same applies for $K_5Na[Ce_2(SO_4)_6]$ and $K_6[Ce_2(SO_4)_6]$. Since within equivalent pairs of Ln-elements in these structures average Ln-O distances are identical, we can now look at the overall trend between the six lanthanide elements presented. LnO_{10} average bond distances between La and Eu confirm the trend we just discussed for Ce and Pr, with average distances for LaO_{10} = 2.614 Å, CeO_{10} = 2.604 Å, PrO_{10} = 2.584 Å, NdO_{10} = 2.571 Å, SmO_{10} = 2.545 Å, and EuO_{10} = 2.535 Å. All bond valence sums hover around 2.8 confirming a formal oxidation state of +3 for all lanthanides within this set of compounds.

The 2D-layers extending within the *ab*-plane are tied together along the *c*-axis via 9 and 8 -coordinate K^+-ions and 6-coordinate Na^+-ions (Figure 4). The K(1)-central atoms are surrounded by six sulfate tetrahedra forming KO_9-coordination polyhedra. Half of the tetrahedra bind in a bidentate and the other half in a monodentate mode. The eight coordinating oxygen atoms around the K(2) metal centers stem from four sulfate tetrahedra, all of which coordinate in bidentate fashion (Figure 5A). In contrast, the smaller sodium cations are surrounded by six sulfate entities that all bind in a monodentate style resulting in NaO_6-coordination polyhedra (Figure 5B). The Na-metal centers lie on the mirror plane that coincides with the *ac*-plane, while K(2)-atoms lie on both mirror planes. K(2) in **1** as well as in all the previously reported $K_5Na[Ln_2(SO_4)_6]$ isomorphs has a relatively large, asymmetric atomic displacement parameter (ADP), much larger than for all other atoms in their respective structures. A potential reason for this could be the fact that K(2) is located on the two mirror planes as well as a two-fold axis, which could cause the formation of several degenerated energy minima, with the actual atom positions slightly displaced away from the special position towards some of the coordinating O-atoms, and away from others, causing disorder for K(2) (either static, if the degenerate minima are separated by a sufficiently high energy barrier, or dynamic, if interconversion is not hindered). When added up, these degenerate positions could give the appearance of an asymmetric ADP. If pronounced enough, the displacement could be refined as disorder, which had been done in $K_5Na[Nd_2(SO_4)_6]$ as well as $K_6[Pr_2(SO_4)_6]$ and $K_6[Ce_2(SO_4)_6]$.[31] In the $K_6[La_2(SO_4)_6]$ equivalent K(2) was however not refined as disordered, but the atom has instead a rather large asymmetric ADP.[31] For $K_5Na[Pr_2(SO_4)_6]$, the title compound, we have also chosen to not refine disorder. Since CN = 8 for K(2) as compared to CN = 9 for K(1) it seems that K(2) has more space available for displacement or disorder within the center of its coordination polyhedron. For K(3) in the $K_6[Ln_2(SO_4)_6]$ series CN = 6 and, thus, these potassium atoms truly occupy the position of the smaller Na-atoms in the $K_5Na[Pr_2(SO_4)_6]$ structure, and no signs for disorder are observed. In Table 3 we list the K(3)-O and the Na-O average bond distances of the $K(3)O_6$ and NaO_6-octahedra, which compare very well.

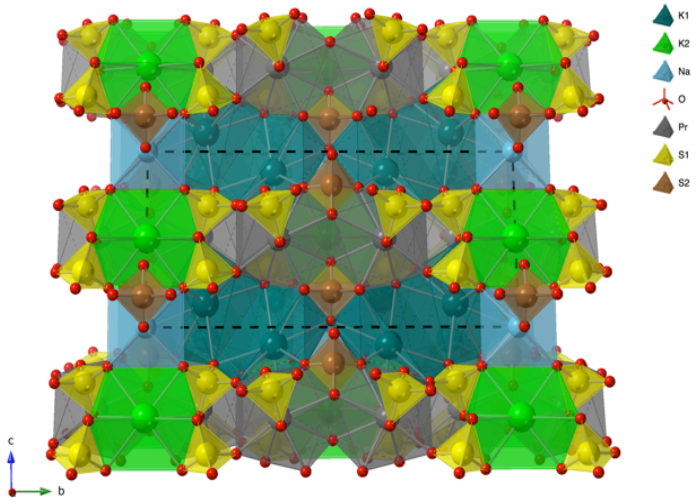

Figure 4: View onto the *bc*-plane of **1**, illustrating how 2D-layers of Pr_2O_{18}-coordination polyhedra interlinked via SO_4-tetrahedra are tied together via 9 and 8 -coordinate K-metal centers and 6-coordinate Na^+-ions.

It seems that the trend of decreasing bond distances is rather small for these octahedral coordination spheres with average bond lengths for $K(3)O_6$ = 2.365 Å (K_6-La), 2.364 Å, (K_6-Ce), NaO_6 = 2.368 Å, (K_5Na-Ce), $K(3)O_6$ = 2.357 Å, (K_6-Pr), NaO_6 = 2.354 Å, (K_5Na-Pr), 2.355 Å, (K_5Na-Nd), 2.344 Å, (K_5Na-Sm), and 2.343 Å, (K_5Na-Eu).

Table 4 shows the average bond distances for the K(1) O_9-polyhedra and Table 5 lists the average bond lengths for the $K(2)O_8$-polyhedra. The trends of the average bond lengths for the $K(1)O_9$ and $K(2)O_8$ -polyhedra lie within the expected range.

Conclusion

Our work contributes data to a series of previously published 10-coordinate lanthanide sulfate networks that integrate K^+ or K^+ and Na^+ into their crystal lattices. The average Ln-O bond distanc-

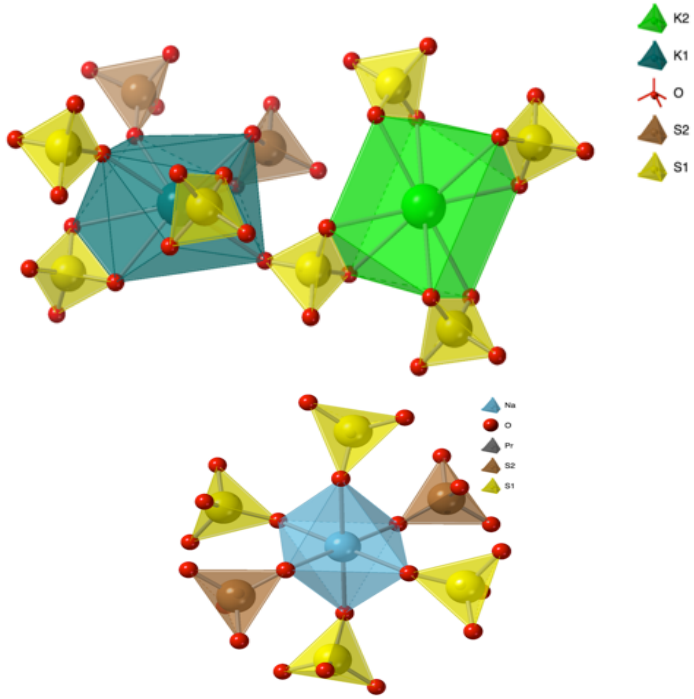

Figure 5. K(1) central atoms assembling as KO_9-coordination polyhedra, surrounded by six sulfate tetrahedra. Three sulfate entities bind in a bidentate and the other three in a monodentate mode. The eight coordinating oxygen atoms around the K(2)-metal centers originate from four sulfate ions, which coordinate in a bidentate fashion (A). Smaller sodium cations are surrounded by six sulfate ions, all binding in a monodentate style producing NaO_6-coordination polyhedra (B).

es within LnO_{10}-coordination polyhedra in $K_6[Pr_2(SO_4)_6]$ reported by Sørensen et al. and in our title compound, $K_5Na[Pr_2(SO_4)_6]$, are equivalent. They share the structural motif of the infinitely interlinked Pr_2O_{18}-coordination polyhedra via sulfate ions within the *ab*-planes. The same is observed for $K_6[Ce_2(SO_4)_6]$ and $K_5Na[Ce_2(SO_4)_6]$. The only overall structural difference between the two pairs of compounds can be attributed to the various coordination environments of the potassium-metal centers as well as sodium-ions, interlinking the 2D-layers within the *ab*-plane along the *c*-axis. The average Ln-O bond lengths gradually decrease moving from La to Eu, following the trend of decreasing Ln^{3+}-ionic radii along the lanthanide series. Next, we hope to establish a simplified synthetic protocol to produce these networks with phase purity, which should allow us to create isomorphous actinide-coordination networks integrating trivalent Pu and Am respectively.

Table 3. Comparing average bond distances of $K(3)O_6$ and NaO_6-octahedra in $K_6[Ln_2(SO_4)_6]$[31] and $K_5Na[Ln_2(SO_4)_6]$.

$K_6[La_2(SO_4)_6]$ measured at 100 K	Average K(3)-O distances: 2.365 Å Sørensen et al.[31]	$K_5Na[Nd_2(SO_4)_6]$ measured at 150 K	Average Na-O distances: 2.355 Å Sørensen et al.[31]
$K_6[Ce_2(SO_4)_6]$ measured at 100 K	Average K(3)-O distances: 2.364 Å Sørensen et al.[31]	$K_5Na[Ce_2(SO_4)_6]$ measured at 173 K	Average K(3)-O distances: 2.368 Å Erikkson *et* al.[32]
$K_6[Pr_2(SO_4)_6]$ measured at 100 K	Average K(3)-O distances: 2.357 Å Sørensen et al.[31]	$K_5Na[Pr_2(SO_4)_6]$ (**1**) measured at 150 K	Average Na-O distances: 2.354 Å This work
$K_5Na[Sm_2(SO_4)_6]$ measured at 100 K	Average K(3)-O distances: 2.344 Å Sørensen et al.[31]	$K_5Na[Eu_2(SO_4)_6]$ measured at 150 K	Average K(3)-O distances: 2.343 Å Sørensen et al.[31]

Table 4. Comparing average bond distances of $K(1)O_9$-polyhedra in $K_6[Ln_2(SO_4)_6]$[31] and $K_5Na[Ln_2(SO_4)_6]$.

$K_6[La_2(SO_4)_6]$ measured at 100 K	Average K(1)-O distances: 2.844 Å Sørensen et al.[31]	$K_5Na[Nd_2(SO_4)_6]$ measured at 150 K	Average K(1)-O distances: 2.835 Å Sørensen et al.[31]
$K_6[Ce_2(SO_4)_6]$ measured at 100 K	Average K(1)-O distances: 2.836 Å Sørensen et al.[31]	$K_5Na[Ce_2(SO_4)_6]$ measured at 173 K	Average K(1)-O distances: 2.851 Å Erikkson *et* al.[32]
$K_6[Pr_2(SO_4)_6]$ measured at 100 K	Average K(1)-O distances: 2.839 Å Sørensen et al.[31]	$K_5Na[Pr_2(SO_4)_6]$ (**1**) measured at 150 K	Average K(1)-O distances: 2.841 Å This work
$K_6[Sm_2(SO_4)_6]$ measured at 100 K	Average K(1)-O distances: 2.835 Å Sørensen et al.[31]	$K_5Na[Eu_2(SO_4)_6]$ measured at 150 K	Average K(1)-O distances: 2.834 Å Sørensen et al.[31]

Table 5. Comparing average bond distances of $K(2)O_8$-polyhedra in $K_6[Ln_2(SO_4)_6]$[31] and $K_5Na[Ln_2(SO_4)_6]$.

$K_6[La_2(SO_4)_6]$ measured at 100 K Disordered	Average K(2)-O distances: 2.894 Å Sørensen et al.[31]	$K_5Na[Nd_2(SO_4)_6]$ measured at 150 K Disordered	Average K(2)-O distances: 2.873 Å Sørensen et al.[31]
$K_6[Ce_2(SO_4)_6]$ measured at 100 K Disordered	Average K(2)-O distances: 2.894 Å Sørensen et al.[31]	$K_5Na[Ce_2(SO_4)_6]$ measured at 173 K	Average K(2)-O distances: 3.04 Å Erikkson *et* al.[32]
$K_6[Pr_2(SO_4)_6]$ measured at 100 K	Average K(2)-O distances: 2.883Å Sørensen et al.[31]	$K_5Na[Pr_2(SO_4)_6]$ (**1**) measured at 150 K	Average K(2)-O distances: 2.878 Å This work
$K_6[Sm_2(SO_4)_6]$ measured at 100 K	Average K(2)-O distances: 2.856 Å Sørensen et al.[31]	$K_5Na[Eu_2(SO_4)_6]$ measured at 150 K	Average K(2)-O distances: 2.8477 Å Sørensen et al.[31]

Acknowledgements

We would like to thank Angelo State University for funding and providing laboratory space. We further like to thank the Welch Foundation for funding the research conducted at Angelo State University, including the stipends for undergraduate students. Funding for the single crystal X-ray diffractometer at Purdue University was provided by the National Science Foundation through the Major Research Instrumentation Program under Grant No. CHE 1625543.

References

(1). Pravalie, R.; Bandoc, G. *J. Environ. Manage.* **2018**, *209*, 81-92.
(2). Knapp, V.; Pevec, D. *Energ. Policy* **2018**, *120*, 94-99.
(3). Mathew, M. D. *Prog. Nucl. Energ.* **2022**, *143*, 104080-104089.
(4). Velasquez, C. E.; Estanislau, F. B. G. L.; Costa, A. L.; Veloso, M. A. F.; Pereira, C. *Prog. Nucl. Energ.* **2021**, *136*, 103747-10361.
(5). Thorpe, C. L.; Neeway, J. J.; Pearce, C. I.; Hand, R. J.; Fisher, A. J.; Walling, S. A.; Hyatt, N. C.; Kruger, A. A.; Schweiger, M.; Kosson, D. S.; Arendt, C. L.; Marcial, J.; Corkhill, C. L. *npj Mater. Degrad.* **2021**, *5*.
(6). Culea, E.; Negoescu, A.; Cosma, C. *J. Nucl. Mat.* **1994**, *270*, 220-221.
(7). Taylor, R.; Bodel, W.; Stamford, L.; Butler, G. *Energies* **2022**, *15*.
(8). Gupta, H. P.; Menon, S. V. G.; Banerjee, S. *J. Nucl. Mat.* **2008**, *383*, 54-62.
(9). Piet, S. J.; Dixon, B. W.; Jacobson, J. J.; Matthern, G. E.; Shropshire, D. E. *Nucl. Technol.* **2017**, *173*, 227-238.
(10). Lee, W. E.; Ojovan, M. I.; Stennett, M. C.; Hyatt, N. C. *Adv. Appl. Ceram.* **2013**, *105*, 3-12.
(11). Sullivan, G. K. *Ceram. Trans.* **1995**, *61*, 187-193.
(12). Ewing, R. C. *Natl. Acad. Sci. USA* **1999**, *96*, 3432-3439.
(13). Wang, S. A., E.; Ling, J.; Skanthakumar, S.; Soderholm, L.; Depmeier, W.; Albrecht-Schmitt, T. *Angew. Chem. Int. Ed.* **2010**, *49*, 1263-1266.
(14). Lv, K.; Fichter, S.; Gu, M.; März, J.; Schmidt, M. *Coord. Chem. Rev.* **2021**, *446*.
(15). Hastings, A. M.; Ray, D.; Jeong, W.; Gagliardi, L.; Farha, O. K.; Hixon, A. E. *J. Am. Chem. Soc.* **2020**, *142*, 9363-9371.
(16). Dolgopolova, E. A.; Rice, A. M.; Shustova, N. B. *Chem. Commun.* **2018**, *54*, 6472-6483.
(17). Schleid, T. M., L.R.; Meyer, G. *J. Less-Common Met.* **1987**, *127*, 183-187.
(18). Peterson, J. R.; Cunningham, B. B. *J. Inorg. and Nucl. Chem.* **1968**, *30*, 823-828.
(19). Fujita, D. K.; Cunningham, B. B.; Parsons, T. C. *Inorg. Nucl.*

Chem. Lett. **1969**, *5*, 307-313.
(20). Zehnder, R. A.; Clark, D. L.; Scott, B. L.; Donohoe, R. J.; Palmer, P. D.; Runde, W. H.; Hobart, D. E. *Inorg. Chem.* **2010**, *49*, 4781-4790.
(21). Zehnder, R. A.; Fontaine, N. C.; Zeller, M.; Renn, R. A. *Acta Cryst.* **2010**, *C66*, m371-m374.
(22). Zehnder, R. A.; Wilson, C. S.; Christy, H. T.; Harris, K. S.; Chauhan, V.; Schutz, V.; Sullivan, M.; Zeller, M.; Fronczek, F. R.; Myers, J. A.; Dammann, K.; Duck, J.; Smith, P. M.; Okuma, A.; Johnson, K.; Sovesky, R.; Stroudt, C.; Renn, R. A. *Inorg. Chem.* **2011**, *50*, 836-46.
(23). Zehnder, R. A.; Renn, R. A.; Pippin, E.; Zeller, M.; Wheeler, K. A.; Carr, J. A.; Fontaine, N.; McMullen, N. C. *J. Mol. Struct.* **2011**, *985*, 109-119.
(24). *Bruker (2022). Apex4 2022.1-1, SAINT V8.40B, Bruker AXS Inc.: Madison (WI), USA,* **2022**.
(25). Krause, L.; Herbst-Irmer, R.; Sheldrick, G. M.; D., S. *J. Appl. Cryst.* **2015**, *48*, 3-10.
(26). SHELXTL suite of programs, Version 6.14, Bruker Advanced X-ray Solutions, Bruker AXS Inc., Madison, Wisconsin: *USA.,* **2000-2003**.
(27). Sheldrick, G. M. *Acta. Cryst.* **2008**, *A 64*, 112-122.
(28). Sheldrick, G. M. *Acta Cryst.* **2015**, *C71*, 3-8.
(29). Sheldrick, G. M., Germany, SHELXL-2019, Universität Göttingen, Göttingen, Germany, **2018**.
(30). Storm Thomsen, M.; Anker, A. S.; Kacenauskaite, L.; Sørensen, T. J. *Dalton Trans.* **2022**, *51*, 8960-8963.
(31). Storm Thomsen, M.; Sørensen, T. J. *Dalton Trans.* **2022**, *51*, 8964-8974.
(32). Eriksson, A. K.; Casari, B. M.; Langer, V. *Acta Cryst.* **2003**, *E59*, i149-i150.
(33). Brown, I. D., Altermatt, D. *Acta Cryst.* **1985**, *B41*, 244-247.
(34). Brown, D. A. *Bond valence parameters,* McMaster University, Hamilton, Ontario, Canada, **2020**.
(35). Garcia-Rodriguez, L. R.-P., A.; Pinero, J. R.; Gonzalez-Silgo, C. *Acta Cryst.* **2000**, *B56*, 665-669.
(36). Brown, I. D. *Acta Cryst.* **1992**, *B48*, 553.
(37). Nguyen, T. N. Helen Scientific Research and Technological Development Co., Ltd, Ho Chi Minh City, Vietnam, **1-10**.